Zero-Crossing Detection Frequency Estimator Method Combined with a Kalman Filter for Non-ideal Power Grid

Tiago Davi Curi Busarello
Department of Engineering
Federal University of Santa Catarina
Blumenau - Brazil
tiago.busarello@ufsc.br

Sérgio Luiz Sambugari Junior
Departamento de Engenharia Elétrica
Universidade Estadual de Londrina
Londrina, Brazil
slsj08@gmail.com

Newton da Silva
Departamento de Engenharia Elétrica
Universidade Estadual de Londrina
Londrina, Brazil
newton.silva@uel.br

***Abstract*—This paper proposes a Zero-Crossing Detection Frequency Estimator Method combined with a Kalman Filter for Non-ideal Power Grid. The Kalman filter generates the in-phase and in-quadrature signals from the voltage grid. Due to the adaptive feature of the Kalman figure, the in-phase and in-quadrature signals are free of noise and harmonics and it guarantees an accurate frequency estimation for a long range of grid frequency. With both clean signals in-phase and in-quadrature, the frequency estimator computes the arc tangent of the relationship between them. The result is a ramp signal varying from -pi to +pi. Such a signal is used to estimate the frequency. Considering zero-crossing detection, the frequency estimator counts the number of samples within a fundamental period. Experimental results show the efficacy of the proposed method. The frequency estimator was implemented C2000 Delfino MCU F28379D LaunchPad development kit.**

Keywords—Frequency estimator, Kalman Filter, F28379D LaunchPad, Power grid, PLL, distorted voltage.

I. Introduction

Measurements of electrical variables in a power grid is being obtained since the beginning of first installations of the electric sector. For a long time, such measurements were easy and most of them were clean signals. With the advancement of electronic technology, several disturbances that were once unworried are now causing problems for an accurate measurement. The grid frequency which hardly deviated from its nominal value is nowadays suffering vast variations due to occurrences like connection of distributed generators and nonlinear loads with intermittent behavior [1].

Measuring the grid frequency has an important and indispensable role for system operators. The value of the frequency may be used in algorithms designated to manage the grid, to decide the best power dispatch of generators, to stabilize the grid and so on. Therefore, there is a need for an accurate, fast and reliable measurement of the grid frequency. Deviation from the normal condition such as the presence of noise and harmonic, sudden changes in phase and amplitude cannot compromise the frequency measurements.

The grid frequency value is not directly measured. It is necessary an indirect method. Therefore, the frequency is estimated. For this reason, it is common to say frequency estimation instead of frequency measurement. Frequency estimation methods are constantly being reported in the literature [2]–[13]. In [2] the authors proposed an approach using a novel circular limit cycle oscillator (CLO) coupled with frequency-locked loop (FLL). Due to the nonlinear structure of the CLO, the proposed frequency adaptive CLO technique is robust against various perturbations faced in the practical settings like discontinuous jump of phase, frequency and amplitude. In [3] the proposal is about an adaptive sliding mode observer for frequency and phase estimation. The observer is simple, easy to tune and suitable for real-time implementation.

A Fourier Transform-Based Frequency Estimation Algorithm is proposed in [4] where the algorithm is a modified synchronous clock generator that together with a modified frequency interpolation method provides an accurate measurement of the input signal frequency when the only available information about the sampling clock is a given integer multiple of the input signal fundamental frequency. In [10], similar Fourier-Based transform algorithm shows a wide frequency range applicability.

Frequency estimation methods are also found in solution based on Phase-Locked Loop (PLL) [14]–[18]. Knowing the frequency value of the grid is also essential in power electronics application like grid-connected converters [19]–[22].

All the above-mentioned researches have their efficacy and legitimacy. However, new issues can be addressed. This paper proposes a Zero-Crossing Detection Frequency Estimator Method using Kalman Filter for Non-ideal Power Grid. The Kalman filter generates the in-phase and in-quadrature signals from the voltage grid. Due to the adaptive feature of the Kalman figure, the in-phase and in-quadrature signals are free of noise and harmonics and it guarantees an accurate frequency estimation for a long range of grid frequency. With both clean signals in-phase and in-quadrature, the frequency estimator computes the arc tangent of the relationship between them. The result is a ramp signal varying from $-\pi$ to $+\pi$. Such a signal is used to estimate the frequency. Considering zero-crossing detection, the frequency estimator counts the number of samples within a fundamental period.

II. The Frequency Estimator Method

Fig. 1 presents a simplified diagram of the proposed Zero-Crossing Detection Frequency Estimator Method using Kalman Filter. The grid voltage is the input signal (z). This signal passes through the Kalman filter, which in turn, produces two filtered signals ($\hat{x}_1 and\ \hat{x}_2$). These signals are the estimated fundamental frequency component of the input signal and its orthogonal component. Later, these signals are

The authors thank to National Council for Scientific and Technological Development – CNPq (grant 421281/2016- 2).

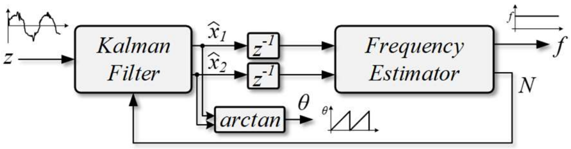

Fig. 1. Simplified diagram of the proposed Zero-Crossing Detection Frequency Estimator Method using Kalman Filter.

sent to the frequency estimator block. The unit delay blocks are necessary to avoid algebraic loop. The frequency is estimated with a method based on the zero-crossing detection. The arc tangent of the filtered signals is computed and a ramp signal varying from $-\pi$ to $+\pi$ is obtained. The number of samples is then computed (*N*) in one period of the input signal and then sent it back to the Kalman filter. This assures a satisfactory performance over a large input signal frequency range. The value of *N* depends on the frequency of the input signal. The value of theta θ can be computed by taking the arctan of signals $\hat{x}_1 and\ \hat{x}_2$. Actually, such computation is done within the block of Frequency Estimator. The arctan is shown outside for the sake of simplicity. The result of this operation is the phase angle of the input signal. Therefore, the proposed zero-crossing detection frequency estimator method using Kalman Filter may also be used as PLL.

III. Background on Kalman Filtering

The Kalman filter estimates a state of a linear system in the presence of uncertainties, noise and inaccurate measurement. This ability of estimating a state is due to a recursive method where the goal is to minimize the sum of squares of the difference between the real and estimated values. Such a method has two processes: prediction and estimation.

The prediction is also known as prior estimate. It estimates the current state taking into account the estimate and error covariance of the previous step. The prediction process does not consider the current input data of the Kalman filter. Later, the estimation process uses the prediction values to update the current state.

A linear system can be modeled in state-space equations such as:

$$\begin{cases} x_k = A_k x_{k-1} + w_k \\ z_k = H_k x_k + v_k \end{cases} \quad (1)$$

where:

$$\begin{aligned} &k \text{ is the current state} \\ &x_k \text{ the state at } t = k \\ &w_k \text{ is the noise of the process} \\ &z_k \text{ is the state observation at } t = k \\ &v_k \text{ is the noise of the measurments} \\ &A_k \ and\ H_k \text{ are the inputs of the system} \end{aligned} \quad (2)$$

The noises w_k and v_k are white band-limited Gaussian noises with zero average. Moreover, the noises have covariance Q_k and R_k. Therefore, the noises are described by:

$$\begin{cases} w_k \sim N(0, Q_k) \\ v_k \sim N(0, R_k) \end{cases} \quad (3)$$

In order to compute the state at *t*= *k*, the Kalman filter computes the following set of equations. The first is the definition of the initial values for the estimate and the error covariance, given by:

$$\hat{x}_0, P_0 \quad (4)$$

The next step of the algorithm consist of two parts. The first is the computation of the state prediction, given by:

$$\hat{x}_k^- = A\hat{x}_{k-1} \quad (5)$$

The superscipt $^-$ means prediction. The second part is the computation of the covariance error prediction, given by:

$$P_k^- = AP_{k-1}A^T + Q \quad (6)$$

Where P_k^- is the covariance error prediction.

The next step is the computation of the Kalman gain (*K*), given by:

$$K_k = P_k^- H^T \left(HP_k^- H^T + R \right)^{-1} \quad (7)$$

The estimate of the state is the next computation, given by:

$$\hat{x}_k = \hat{x}_k^- + K_k \left(z_k - H\hat{x}_k^- \right) \quad (8)$$

Notice that (8) is the only equation where the state observation is used.

After computing the estimate, the error covariance must be computed in order to be used in the next prediction. The error covariance is given by:

$$P_k = P_k^- - K_k H P_k^- \quad (9)$$

IV. System Modeling

In order to estimate the fundamental frequency in a non-ideal power grid, the power grid must be modeled in state-space equations, containing dynamic behavior as well as possible noise in the grid.

Considering initially a sinusoidal voltage given by:

$$x_k = M_k \sin\left(\omega_k t_k + \theta_k\right) \quad (10)$$

where M_k in amplitude, ω_k is angular frequency, θ_k is phase angle and t_k is time at instant *k*.

Considering also two orthogonal signals, x_{1k} and x_{2k}, given by:

$$\begin{cases} x_{1k} = M_k \sin\left(\omega_k t_k + \theta_k\right) \\ x_{2k} = M_k \cos\left(\omega_k t_k + \theta_k\right) \end{cases} \quad (11)$$

If $M_k \approx M_{k+1}$, $\omega_k \approx \omega_{k+1}$, $\theta_k \approx \theta_{k+1}$ and $t_{k+1} \approx t_k + T_s$ with T_s the sampling period, one may find:

$$\begin{cases} x_{1_{k+1}} = M_k \sin\left(\omega_k t_k + \omega_k T_s + \theta_k\right) \\ x_{2_{k+1}} = M_k \cos\left(\omega_k t_k + \omega_k T_s + \theta_k\right) \end{cases} \quad (12)$$

Resulting in:

$$\begin{cases} x_{1_{k+1}} = x_{1k}\cos(\omega_k T_s) + x_{2k}\sin(\omega_k T_s) \\ x_{2_{k+1}} = -x_{1k}\sin(\omega_k T_s) + x_{2k}\cos(\omega_k T_s) \end{cases} \quad (13)$$

Writing (13) using matrix, it results:

$$\begin{bmatrix} x_1 \\ x_2 \end{bmatrix}_{k+1} = \begin{bmatrix} \cos(\omega_k T_s) & \sin(\omega_k T_s) \\ -\sin(\omega_k T_s) & \cos(\omega_k T_s) \end{bmatrix} \begin{bmatrix} x_1 \\ x_2 \end{bmatrix}_k \quad (14)$$

Taking into account the noise of the measurements and process w_k and v_k, respectively, the non-ideal power grid is modeled in state-space equations as:

$$\begin{bmatrix} x_1 \\ x_2 \end{bmatrix}_{k+1} = \begin{bmatrix} \cos(\omega_k T_s) & \sin(\omega_k T_s) \\ -\sin(\omega_k T_s) & \cos(\omega_k T_s) \end{bmatrix} \begin{bmatrix} x_1 \\ x_2 \end{bmatrix}_k + \begin{bmatrix} w_1 \\ w_2 \end{bmatrix}_k \quad (15)$$

$$z_k = \begin{bmatrix} 0 & 1 \end{bmatrix} \begin{bmatrix} x_1 \\ x_2 \end{bmatrix}_k + v_k \quad (16)$$

With (15) and (16) it is possible to apply the Kalman filter and estimate the fundamental component of voltage of the non-ideal power grid, even though the voltage has noise and harmonic distortion.

V. Frequency Estimation

The frequency estimator block of Fig. 1 estimates the frequency based on a zero-crossing detection and the relationship between the frequency of the input signal and the number of samples.

The number of samples is calculated according to:

$$N = \frac{f_s}{f_{signal}} = \frac{T_{signal}}{T_s} \quad (17)$$

where f_s is the sampling frequency and f_{signal} is the frequency of the input signal.

In order to detect the number of samples, it would be enough to use the input signal. However, the presence of uncertainties, noise and disturbance in the input signal, the frequency is better estimated with the filtered signal from the Kalman filter.

The number of samples plays an important role in the Kalman filter. This value is used in the matrix $\boldsymbol{A}$ of the Kalman filter, which is updated in every sampling period. Depending on the frequency of the input signal, a value of N is obtained. For an input signal at 60 Hz, the value of N is 200. It means that the 360 degree of one cycle of the input signal is divided into 200 samples. As a result, each sample corresponds to 1.8 degree. In case the input signal changes its frequency from 60 Hz to 50 Hz, the value of N is updated to 240. Consequently, each sample corresponds to 1.5 degree. The updated value of N is feedback to the Kalman filter. Therefore, matrix $\boldsymbol{A}$ is updated every time a change happens in the frequency of the input signal. This shows the efficacy of the proposed frequency estimation method for non-ideal power grid.

The instantaneous angle is given by:

$$\theta_k = \arctan\left(-\frac{x_{1k}}{x_{2k}}\right) \quad (18)$$

Eq. (18) is variable in time. The theta is the ramp signal mentioned previously. From this signal, the number of samples is calculated. The value of N begins to be counted in a zero-cross of the theta signal. The counting ends in the next zero-crossing. Notice that since the in-phase and in-quadrature signal are clean signals due to the Kalman filter, the computation of N has accuracy on is value.

VI. Experimental Results

The proposed frequency estimator method of Fig. 1 was experimentally verified in the Digital Signal Controller (DSC) C2000 Delfino MCU F28379D LaunchPad development kit. Tab. I presents the parameters of the prototype. The results were collected through the Digital-Analog Converter (DAC) of the DSC.

Fig. 2 presents the input signal (z), which is also known as measurement, and the output signals of the Kalman filter ($\hat{x}_1 and\ \hat{x}_2$). The input signal is a sinusoidal waveform with amplitude equals to 1.5 V and the frequency is 60 Hz. The ($\hat{x}_1$) is in-phase with the input signal while the ($\hat{x}_2$) is in-quadrature. The Kalman filter produces the in-phase and in-quadrature signals orthogonal related to each other.

TABLE I. Parameters of the Prototype

Parameter	Value
Matrix A	$A = \begin{bmatrix} \cos(\pi/N) & -\sin(\pi/N) \\ \sin(\pi/N) & \cos(\pi/N) \end{bmatrix}$
Matrix H	$H = \begin{bmatrix} 1 & 0 \end{bmatrix}$
Matrix Q	$Q = \begin{bmatrix} 0.01 & 0 \\ 0 & 0.01 \end{bmatrix}$
Matrix R	$R = 25$
Matrix $\hat{x}_0$	$\hat{x}_0 = \begin{bmatrix} 0 & 0 \end{bmatrix}$
Matrix P_0	$P_0 = \begin{bmatrix} 1 & 0 \\ 0 & 1 \end{bmatrix}$
Sampling Frequency	*12 kHz*

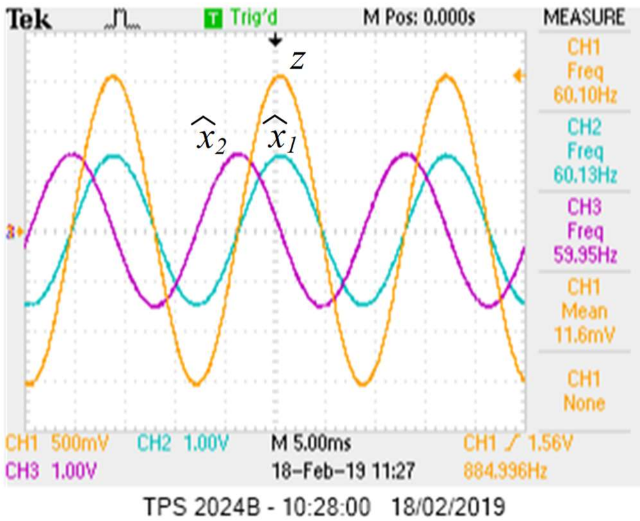

Fig. 2. The input signal (z) and the output signals of the Kalman filter ($\hat{x}_1 and\ \hat{x}_2$).

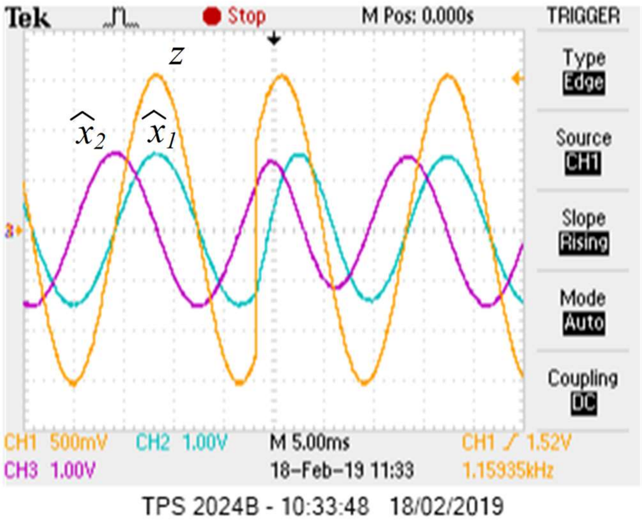

Fig. 3. The input signal (z) and the output signals of the Kalman filter $(\hat{x}_1 and\ \hat{x}_2)$ when the input signal suffers a 90 degrees phase shift.

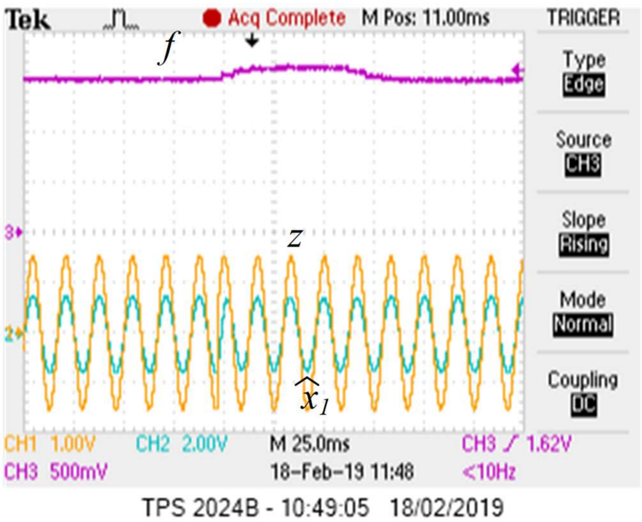

Fig. 4. The estimated frequency (f), the input signal (z) and the in-phase signal when the input signal $(\hat{x}_1)$ suffers a 90 degrees phase shif (CH3: 500 mV/ 20 Hz).

Fig. 3 presents input signal (z) and the output signals of the Kalman filter $(\hat{x}_1 and\ \hat{x}_2)$ when the input signal suffers a 90 degrees phase shift. Before the phase shift, the signals are in accordance to that presented in the previous figure. After the phase shift, the in-phase and in-quadrature signals of the Kalman filter reach steady-state in less than one fundamental cycle of the input signal. In other words, the in-phase signal in again in-phase with the input signal in less than one cycle.

Fig. 4 presents the estimated frequency (f), the input signal (z) and the in-phase signal when the input signal $(\hat{x}_1)$ suffers a 90 degrees phase shift. The estimated frequency returns to its steady-state value in approximately 75 ms after the phase shift.

Fig. 5 presents the estimated frequency (f), the input signal (z) and the in-phase signal when the input signal $(\hat{x}_1)$ changes

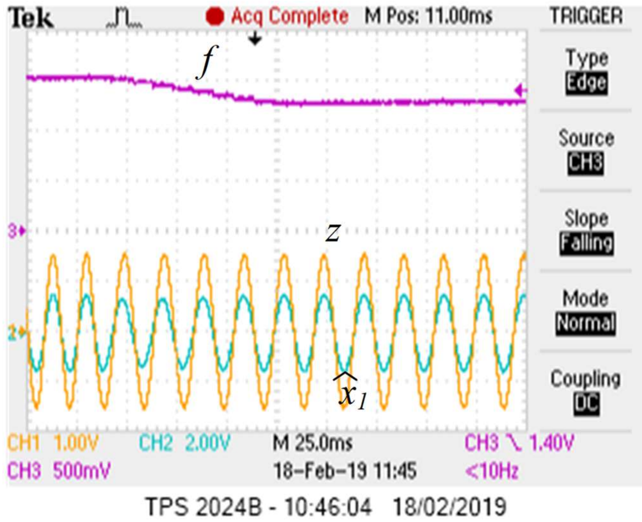

Fig. 5. The estimated frequency (f), the input signal (z) and the in-phase signal when the input signal $(\hat{x}_1)$ changes from 60 Hz to 50 Hz (CH3: 500 mV/ 20 Hz).

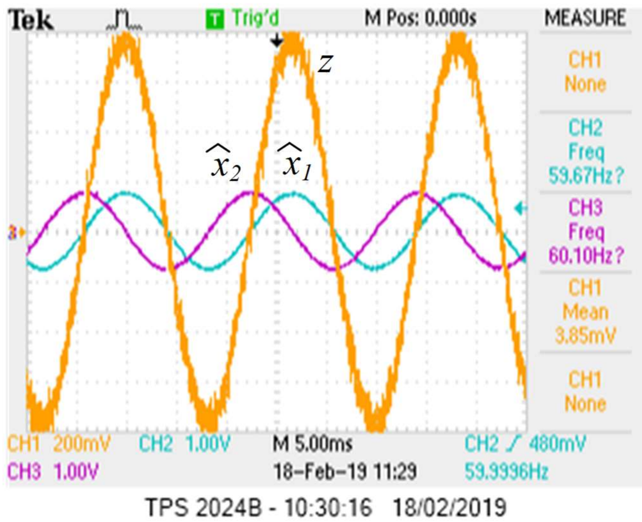

Fig. 6. The input signal (z) and the output signals of the Kalman filter $(\hat{x}_1 and\ \hat{x}_2)$ when the input signal is polluted with noise.

from 50 Hz to 60 Hz. The estimated frequency reaches the steady-state condition after approximately 60 ms. The estimated frequency signal did not present neither oscillatory nor unpredictable behavior.

Fig. 6 presents the input signal (z) and the output signals of the Kalman filter $(\hat{x}_1 and\ \hat{x}_2)$ when the input signal is polluted with noise. The in-phase and in-quadrature signal $(\hat{x}_1 and\ \hat{x}_2)$ are free of noise and they are in-phase and in-quadrature related to the input signal. This result shows the filtering efficacy of the Kalman.

Fig. 7 presents the estimated frequency (f), the input signal (z) and the in-phase signal $(\hat{x}_1)$ at the moment the input signal is polluted with noise. The amplitude of the input signal is also reduced to half. The estimated frequency keeps unchanged on

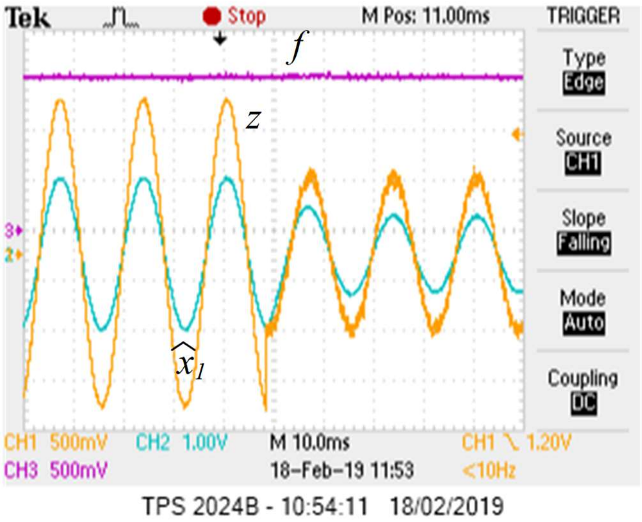

Fig. 7. The estimated frequency (*f*), the input signal (*z*) and the in-phase signal $(\hat{x}_1)$ at the moment the input signal is polluted with noise (CH3: 500 mV/ 20 Hz).

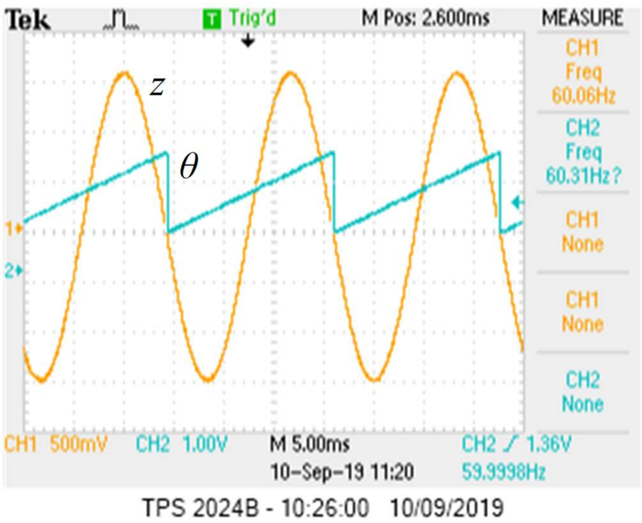

Fig. 8. The input signal (*z*) and the theta signal (θ).

its steady-state value, showing the efficacy of the proposed estimation method.

Fig. 8 presents the input signal (*z*) and the theta signal (θ). The theta signal is synchronized with the input signal. This result shows that the proposed frequency estimator method can also be used as PLL. The values varies from $-\pi$ to $+\pi$ but the result shows a signal with offset due to the range of the DAC.

Fig. 9 presents the input signal (*z*) and the theta signal (θ) when the input signal is polluted with noise. Even in this case, the theta signal is synchronized with the input signal.

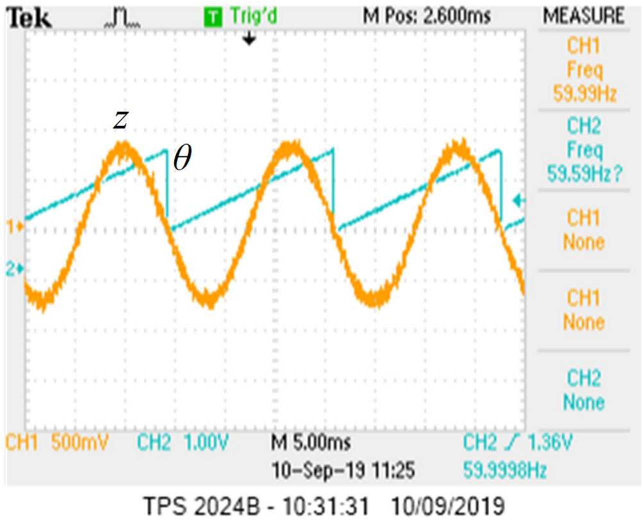

Fig. 9. The input signal (*z*) and the theta signal (θ) when the input signal is polluted with noise.

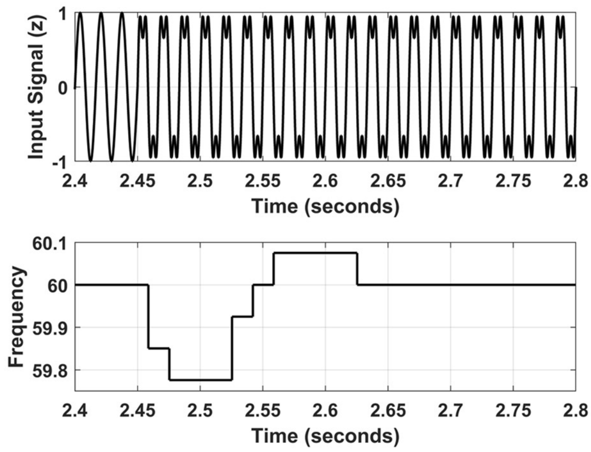

Fig. 10. Simulated result for he input signal (*z*) (at the top) and the estimated frequency (*f*) during the inclusion of harmonic distortion in the input signal.

Fig. 10 presents a simulated result for the input signal (*z*) and the estimated frequency (*f*) during the inclusion of harmonic distortion in the input signal. Initially, the input signal is sinusoidal. At t = 2.45, a third harmonic component (180 Hz) with amplitude equals to 0.35 is added to the input signal. The estimated frequency varies and returns to 60 Hz after a short transient time. This result was presented through simulation due to the incapability of the signal generator to produce such a signal. The value of 0.35 corresponds to 35% of the fundamental component. This value is not practical in voltage power grid, but it was set in this study only to show the efficacy of the proposed frequency estimator.

Fig. 11 presents a picture of the DSP, signal generator and the oscilloscope used to verify experimentally the proposed frequency estimator method.

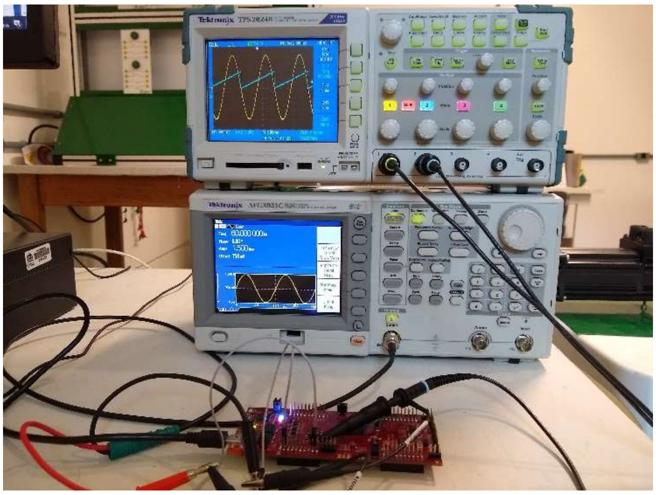

Fig. 11. picture of the DSP, signal generator and the oscilloscope used to verify experimentally the proposed frequency estimator method.

The computational effort and cost of implementing the proposed zero-crossing detection frequency estimator method using Kalman Filter for non-ideal power grid is beyond the scope of this paper, but may be presented by these authors in a future paper.

VII. Conclusion

This paper presented a Zero-Crossing Detection Frequency Estimator Method using Kalman Filter for Non-ideal Power Grid. The Kalman filter generated the in-phase and in-quadrature signals from the voltage grid. Due to the adaptive feature of the Kalman figure, the in-phase and in-quadrature signals were free of noise and harmonics.

Experimental results collected in C2000 Delfino MCU F28379D LaunchPad development kit showed the efficacy of the proposed frequency estimator method. The proposed method was verified under the application of phase displacement, frequency variation and inclusion of noise in the input signal. For all cases, the estimated frequency did not present neither oscillatory nor unpredictable behavior. Therefore, the proposed frequency estimator method based on Kalman filter is an attractive solution to estimating the frequency value of a non-ideal power grid. The simulation files used in this paper is freely available on the author's webpage http://busarello.prof.ufsc.br.

References

[1] M. H. Bollen, *Integration of Distributed Generation in the Power System*. John Wiley & Sons, 2011.

[2] H. Ahmed, S. Amamra, e M. H. Bierhoff, "Frequency-Locked Loop Based Estimation of Single-Phase Grid Voltage Parameters", *IEEE Transactions on Industrial Electronics*, p. 1–1, 2018.

[3] H. Ahmed, S. Amamra, e I. Salgado, "Fast Estimation of Phase and Frequency for Single Phase Grid Signal", *IEEE Transactions on Industrial Electronics*, p. 1–1, 2018.

[4] A. Carboni e A. Ferrero, "A Fourier Transform-Based Frequency Estimation Algorithm", *IEEE Transactions on Instrumentation and Measurement*, vol. 67, nº 7, p. 1722–1728, jul. 2018.

[5] V. Choqueuse, A. Belouchrani, F. Auger, e M. Benbouzid, "Frequency and Phasor Estimations in Three-Phase Systems: Maximum Likelihood Algorithms and Theoretical Performance", *IEEE Transactions on Smart Grid*, p. 1–1, 2018.

[6] Z. Dai, Z. Zhang, Y. Yang, F. Blaabjerg, Y. Huangfu, e J. Zhang, "A Fixed-Length Transfer Delay-based Adaptive Frequency Locked Loop for Single-Phase Systems", *IEEE Transactions on Power Electronics*, p. 1–1, 2018.

[7] J. Li, Z. Teng, Y. Wang, S. You, Y. Liu, e W. Yao, "A Fast Power Grid Frequency Estimation Approach Using Frequency-Shift Filtering", *IEEE Transactions on Power Systems*, p. 1–1, 2019.

[8] S. Tomar e P. Sumathi, "Amplitude and Frequency Estimation of Exponentially Decaying Sinusoids", *IEEE Transactions on Instrumentation and Measurement*, vol. 67, nº 1, p. 229–237, jan. 2018.

[9] H. Wen, C. Li, e W. Yao, "Power System Frequency Estimation of Sine-Wave Corrupted With Noise by Windowed Three-Point Interpolated DFT", *IEEE Transactions on Smart Grid*, vol. 9, nº 5, p. 5163–5172, set. 2018.

[10] L. Zhan, Y. Liu, e Y. Liu, "A Clarke Transformation-Based DFT Phasor and Frequency Algorithm for Wide Frequency Range", *IEEE Transactions on Smart Grid*, vol. 9, nº 1, p. 67–77, jan. 2018.

[11] S. Golestan, J. M. Guerrero, J. C. Vasquez, A. M. Abusorrah, e Y. Al-Turki, "A Study on Three-Phase FLLs", *IEEE Transactions on Power Electronics*, vol. 34, nº 1, p. 213–224, jan. 2019.

[12] M. S. de Padua, "Tecnicas digitais para sincronização com a rede eletrica, com aplicação em geração distribuida", *Dissertação de Metrado - Universidade Estadual de Campinas*, p. 165, 2006.

[13] S. L. S. Junior, "APLICAÇÃO DE FILTRO DE KALMAN PARA FILTRAGEM DE SINAIS DA REDE ELÉTRICA", *Trabalho de Conclusão de Curso - Universidade Estudual de Londrina*, p. 77, 2016.

[14] F. K. A. Lima, R. G. Araujo, F. L. Tofoli, e C. G. C. Branco, "A Phase-Locked Loop Algorithm for Single-Phase Systems with Inherent Disturbance Rejection", *IEEE Transactions on Industrial Electronics*, p. 1–1, 2019.

[15] M. S. Reza, F. Sadeque, M. M. Hossain, A. M. Y. M. Ghias, e V. Agelidis, "Three-Phase PLL for Grid-Connected Power Converters under Both Amplitude and Phase Unbalanced Conditions", *IEEE Transactions on Industrial Electronics*, p. 1–1, 2019.

[16] F. K. de Araújo Lima, R. Guerreiro Araújo, F. L. Tofoli, e C. G. C. Branco, "A three-phase phase-locked loop algorithm with immunity to distorted signals employing an adaptive filter", *Electric Power Systems Research*, vol. 170, p. 116–127, maio 2019.

[17] J. F. Guerreiro, J. A. Pomilio, e T. D. C. Busarello, "Design of a multilevel Active Power Filter for More Electrical Airplane variable frequency systems", in *2013 IEEE Aerospace Conference*, 2013, p. 1–12.

[18] J. F. Guerreiro, J. A. Pomilio, e T. D. C. Busarello, "Design and implementation of a multilevel active power filter for more electric aircraft variable frequency systems", in *2013 Brazilian Power Electronics Conference*, 2013, p. 1001–1007.

[19] M. Babakmehr, F. Harirchi, A. A. Durra, S. M. Muyeen, e M. G. Simões, "Exploiting Compressive System Identification for Multiple Line Outage Detection in Smart Grids", in *2018 IEEE Industry Applications Society Annual Meeting (IAS)*, 2018, p. 1–8.

[20] H. Sartipizadeh e F. Harirchi, "Robust Model Predictive Control of DC-DC Floating Interleaved Boost Converter under Uncertainty", in *2017 Ninth Annual IEEE Green Technologies Conference (GreenTech)*, 2017, p. 320–327.

[21] M. Babakmehr, F. Harirchi, A. Alsaleem, A. Bubshait, e M. G. Simões, "Designing an intelligent low power residential PV-based Microgrid", in *2016 IEEE Industry Applications Society Annual Meeting*, 2016, p. 1–8.

[22] F. Harirchi, M. G. Simões, M. Babakmehr, A. AlDurra, S. M. Muyeen, e A. Bubshait, "Multi-functional double mode inverter for power quality enhancement in smart-grid applications", in *2016 IEEE Industry Applications Society Annual Meeting*, 2016, p. 1–8.